

Taylor & Francis
Taylor & Francis Group

Numerical Heat Transfer, Part A: Applications
An International Journal of Computation and Methodology

ISSN: 1040-7782 (Print) 1521-0634 (Online) Journal homepage: www.tandfonline.com/journals/unht20

Numerical spectral approach for studying activation energy behavior in viscoelastic fluid flow through non-Darcian medium

Anwar Shahid, Wang Wei, T. Abbas, M. M. Bhatti, A. Zeeshan & Khurram Javid

To cite this article: Anwar Shahid, Wang Wei, T. Abbas, M. M. Bhatti, A. Zeeshan & Khurram Javid (2025) Numerical spectral approach for studying activation energy behavior in viscoelastic fluid flow through non-Darcian medium, Numerical Heat Transfer, Part A: Applications, 86:18, 6349-6363, DOI: 10.1080/10407782.2024.2343030

To link to this article: https://doi.org/10.1080/10407782.2024.2343030

Published online: 21 Apr 2024.

Submit your article to this journal

Article views: 122

View related articles

View Crossmark data

Citing articles: 4 View citing articles

Full Terms & Conditions of access and use can be found at
https://www.tandfonline.com/action/journalInformation?journalCode=unht20

NUMERICAL HEAT TRANSFER, PART A: APPLICATIONS
2025, VOL. 86, NO. 18, 6349–6363
https://doi.org/10.1080/10407782.2024.2343030

Taylor & Francis
Taylor & Francis Group

Check for updates

Numerical spectral approach for studying activation energy behavior in viscoelastic fluid flow through non-Darcian medium

Anwar Shahid[a], Wang Wei[a], T. Abbas[b], M. M. Bhatti[c,d], A. Zeeshan[e], and Khurram Javid[f]

[a]School of Science, Zhejiang University of Science and Technology, Hangzhou, P.R. China; [b]Department of Mathematics, Division of Science and Technology, University of Education, Lahore, Pakistan; [c]College of Mathematics and Systems Science, Shandong University of Science & Technology, Qingdao, Shandong, P.R. China; [d]Material Science Innovation and Modelling (MaSIM) Research Focus Area, North-West University (Mafikeng Campus), Mmabatho, South Africa; [e]Department of Mathematics and Statistics, International Islamic University, Islamabad, Pakistan; [f]Department of Mathematics, Northern University, Nowshera, KPK, Pakistan

ABSTRACT

The work examines the effects of MHD incompressible viscoelastic fluid under nonlinear thermal radiation while flowing in a non-Darcy porous medium. The utilization of the Darcy-Brinkmann-Forchheimer model has thus been implemented in the formulation of the momentum equation. The study posits the existence of a chemical phenomenon which involves elements *A* and *B* as two chemical species. The diffusion coefficient of chemical species exhibits inequality when considered for viscoelastic fluid. Numerical solutions are generated using SRM, spectral relaxation technique for governing flow problems. The current algorithm is formulated and implemented using the computational software MATLAB. The results exhibit a considerable degree of agreement with formerly established numerical outcomes within the framework of a specific scenario. The observations from this study provide evidence that chemical species *B* operates as a catalyst in a subsurface environment that is oriented horizontally. As a result, the connection between the homogeneous-heterogeneous scheme can be observed in the context of isothermal cubic autocatalytic occurrences and processes of the first order, subsequently. The utilization of the heterogeneous reaction parameter offers notable advantages in reducing the concentration of the bulk-fluid while simultaneously enhancing the concentration of the catalyst situated over the surface. The current findings contribute to the exploration of the computational study of diffusivities in MHD viscoelastic fluid flow. Specifically, this research inquires the effects of nonlinear thermal radiation and homogeneous-heterogeneous reactions.

ARTICLE HISTORY
Received 22 January 2024
Revised 7 April 2024
Accepted 9 April 2024

KEYWORDS
Activation energy; homogeneous–heterogeneous reactions; nonlinear thermal radiation; porous medium; spectral relaxation method (SRM)

1. Introduction

The investigation of fluid flowing past a horizontal stretchable plate has expanded realistic utilizations in diverse sectors, including the pharmaceutical industry (specifically medicinal pharmaceutical technologies), creating polythene and paper, as well as the science of polymer extrusion, fiber

CONTACT M. M. Bhatti mmbhatti@sdust.edu.cn, mubashirme@hotmail.com College of Mathematics and Systems Science, Shandong University of Science & Technology, Qingdao 266590, Shandong, P.R. China.

© 2024 Taylor & Francis Group, LLC

technology, plastic material products, and the cooling of elasticate sheeting, along with in the realms of science and engineering. It is noteworthy to mention that most of the of the aforementioned fluids are materials that display viscous and elastic properties. Cortell [1] described the heat transfer characteristics of a viscoelastic fluid traveling from a stretched plate while encountering both viscous dissipation and thermal radiation. Singh and Agarwal [2] considered the effect of varying thermal conductivity on viscoelastic fluid flowing past an exponentially stretched subsurface. Abolbashari *et al.*, [3] elaborated on the non-Newtonian fluid flowing over a stretched surface. Adegbie *et al.*, [4] study the behavior of a micropolar fluid at a stagnation point on a melting stretching surface with constant vortex viscosity. Sundeep *et al.*, [5] explored the dual solution Jeffrey nanofluid under the input of a chemical reaction and an induced magnetic field over a stretching surface with stagnation point flow. Studies done by Emad and Pop [6] investigated heat transfer and MHD flow on stretching or shrinking surfaces in the vicinity of stagnation points. Various other studies have been conducted for partial slip and viscous dissipation evaluations. The assessments pertaining to the stretchable surfaces have been expounded upon by references. [7–11].

The amount of energy at the minimum level, i.e. necessary for a particle to traverse a series of chemical reactions involving activation energy, is denoted by E. This concept finds applications in numerous fields like oil storage, food processing, geothermal engineering, and chemical engineering mechanochemistry. An analysis of time-dependent phenomena with activation energy, free convection, and a n^{th}-order reaction was studied by Makinde *et al.*, [12]. Further, Williamson nanofluids with activation energy under a time-dependent magnetic field were scrutinized by Hamid *et al.*, [13]. Irfan *et al.*, [14] investigated the effects of nonlinear combined convective and chemical reactions on the flow of three-dimensional radiative Carreau nanofluid, as well as activation energy. Activation energy is included in a number of recent studies in literature; they may be found in the references [15–17].

Objects emit thermal energy, with the magnitude of radiation increasing proportionally with the object's temperature. When two objects of differing temperatures are in proximity to each other, the warmer object will transfer heat to the cooler object until they both attain an equivalent temperature. This proposition has been scientifically set up as the foundational tenet of communications, which is usually regarded as the foundational premise upon that contemporary physical theory of thermal radiation was constructed in nineteenth century. The study focused on by Sandeep *et al.*, [18] aimed to analyze heat transfer in magnetohydrodynamic nanofluid flowing across a shrinking or stretching surface. Similarly, Raju *et al.*, [19] deal with the thermal radiation impact on ferrofluid flowing on a flat plate under an aligned magnetic field. Many of the investigations utilized Taylor series expansion to reduce the nonlinear temperature, thereby cutting down higher-order parts. This simplification renders the nondimensionalization and parametrizing of the thermal radiation modeling a straightforward assignment. Nevertheless, it is pertinent to note that, if understood linearly, the electromagnetic radiation occurring in liquids amid a few industrial processes is not necessarily practical. Furthermore, the Taylor series expansion can't provide detailed information on the impact, which is why the introduction of the nonlinear thermal radiation model has been crucial in providing accurate explanations. In another related study, Animasaun [20] studied micropolar fluid flowing past an unsteady magnetohydrodynamic vertically permeable subsurface that moved from binary mixtures in an optically lean environment. The study incorporated radiative heat flux terms into the energy equation to model thermal radiation among the flowing fluids, expressed as a 4th power of the temperature. The dimensionless equations were attained partly through the application of Taylor series expansion. Wakif and colleagues [21] presented findings on the thermo-physical characteristics of copper water coupled with thermal radiation for minuscule particles. The numerical solution of p.d.es generated by nonlinear flow problems was achieved through the utilization of the G-Chebyshev-G-Lob collocation method. The researchers recorded that the ratio of heat transfer increased for enlarging

initial volumetric fractions of radiation parameters and tiny particles. Several researchers have examined the several phases of thermal radiation, with relevant sources included in references [22–25].

A porous medium is defined as the composition of solid material fibers unified by pores. The advantages of such media lie in their enhanced internal surface area, which proves to be beneficial in thermal power technologies, coating fabrication, and insulation system procedures. Notably, the dissipation range for permeable mediums is significantly larger than that of conventional substrate coatings, resulting in improved heat convection. Furthermore, the complex and convoluted nature of porous substances makes them perfect for filtering and stopping fluidic movements, making them the best way to control culminating movements. To delve deeper into the mechanisms of porous media, researchers such as Izadi *et al.*, [26], Eid and Nafe [27], Ying *et al.*, [28], and Loganathan *et al.*, [29] have investigated various aspects of these materials. In their studies, they used mathematical modeling techniques, such as the Darcy law and Dupuit-Forchheimer modeling, to examine the impact of factors such as slip, magnetic fields, and heat generation on hybrid nanofluids. Furthermore, they presented thermo-hydraulic analyses of salt-based nanofluids moving across pervious absorbable tubes and expressed the priority of the Darcy-Forchheimer models of entropy generation utilizing a third-grade nanofluid. To gain further insight into porosity and Darcy-Forchheimer scheme flow studies, one may refer to the relevant literature [27, 30–34].

A chemical reaction takes place whenever two or more reactants produce a product. Autocatalysis refers to the process where the catalytic properties of the products from a chemical process expedite the chemical reactions. Merkin [35] utilized an order of magnitude and made similar presumptions as Ludwig Prandtl did with the larger Reynolds numbers in Navier-Stoke's equation. Then, he provided straightforward modeling for the interactions between two chemical species and implicating homogeneous and heterogeneous reactants. Mabood *et al.*, [36] studied chemically reacting fluids flowing through a stretchable subsurface. Animasaun [37] undertook an examination of the nth-order reactants in Casson fluid flowing, which encompasses temperature-dependent plastic dynamic viscosity. Pop and Khan [38], on the other hand, scrutinized the dynamics of homogeneous-heterogeneous reactions. The investigation of the electromagnetic radiative Prandtl fluid flowing using the Darcy-Forchheimer substance scheme is scrutinized by Eid *et al.*, [39]. Hina *et al.*, [40] elaborated on the peristaltic propulsion of Johnson-Segelman fluids of nonlinear thermal radiation having reactions of homogeneous and heterogeneous nature.

This study depicts and covers the gap, i.e. examines the movement of MHD viscoelastic fluid passing through a stretchable surface under nonlinear thermal radiation. Furthermore, in non-Newtonian fluids, no effort has been made to discuss the non-equal diffusivities of homogeneous-heterogeneous reactions that arise as they advance toward a stagnation point through a non-Darcian porous medium. Investigations of nonlinear flow problems have been considered for this study. Nondimensional analysis is done by utilizing suitable similarity variables. Transformed governing equations have been resolved numerically by employing SRM. The defining advantage of the SRM algorithm lies in its ability to decompose a complex series of equations into smaller subsystems, which could be processed incrementally with high computational efficiency and effectiveness. Considering other numerical and analytical methods for solving nonlinear problems, the proposed methodology of SRM has demonstrated exceptional accuracy, ease of development, convergence, and efficiency [38]. The graphical behaviors and tabular representation of the impact of specific dimensionless parametric quantities on the profiles of velocity, temperature, and concentration are showcased, along with the demonstration of the friction factor and local Nusselt number.

2. Mathematical modeling

Consider the situation where an incompressible viscoelastic fluid, which conducts electricity consistently, moves toward a stagnation point over a horizontally extended subsurface. Additionally,

it is subjected to reactions that are both homogeneous and heterogeneous in nature. This fluid is flowing through a non-Darcian medium. The depiction of the physical modeling, in conjunction with the $\overline{x}$ -axis and the $\overline{y}$ -axis, can be observed in Figure 1. The stretched subsurface is oriented parallel to the $\overline{x}$ -axis, while the $\overline{y}$ -axis is situated at a perpendicular angle to each other. Magnitude of magnetic Reynolds number is nonsignificant of viscoelastic flow, making an induced magnetic field apparently negligible, however, an applied magnetic field is present B_0. Moreover, the regular section passes by in proximity to the boundary. Sequentially, the temperatures and concentrations neighboring and distant from the elongated surface are denoted by T_w, C_w and C_∞, T_∞. The velocities of stretchable and free-stream flow are represented as $\tilde{u}_w = c\overline{x}$ and $\tilde{u}_e = a\overline{x}$, where c and a are positive constants that specify the stretched segment. The successful progression of a chemical reaction can sometimes necessitate an increased amount of energy owing to the sluggish nature of fluid-molecule collisions. Therefore, energy and concentration equations use an activation energy expression.

It is also considered that there is a presence of homogeneous-heterogeneous reactants between A and$B$ with respect to the flow of viscoelastic fluid toward the stagnation point. Furthermore, the autocatalytic reaction as species is considered to be a catalyst. According to Merkin's [35] hypothesis, there is an isothermal cubic autocatalytic reaction within the boundary layer, which is represented by

$$A + 2B \Rightarrow 3B, \quad \text{rate} = K_c ab^2, \tag{1}$$

This pattern of chemical reaction, specifically a single isothermal first-order reaction, occurs over the catalyst's surface.

$$A \Rightarrow B, \quad rate = K_s a, \tag{2}$$

The concentrations of species A and B are represented by a and b, correspondingly. The coefficients for the rate of the reaction, K_c and K_s, cannot be classified as a consistent value as they incorporate shared parameters that may impact the reaction rate in addition to the concentration, which is explicitly linked in Eqs. (1) and (2). The equations that govern the boundary layer of the aforementioned assumptions are formulated as [35, 41]:

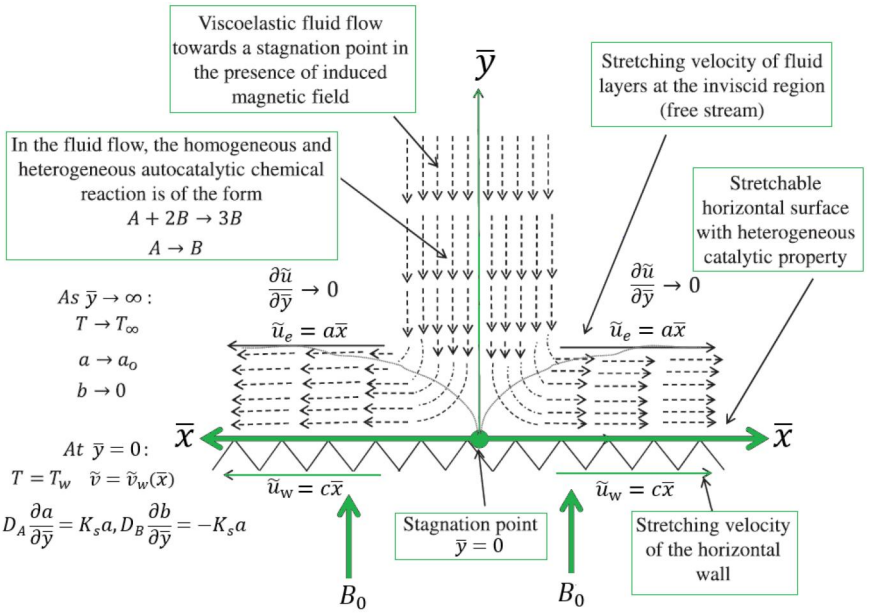


Figure 1. Flow structure and the coordinate system.

$$\frac{\partial \tilde{u}}{\partial \overline{x}} + \frac{\partial \tilde{v}}{\partial \overline{y}} = 0, \tag{3}$$

$$\begin{aligned} \tilde{u}\frac{\partial \tilde{u}}{\partial \overline{x}} + \tilde{v}\frac{\partial \tilde{u}}{\partial \overline{y}} = \tilde{u}_e\frac{\partial \tilde{u}_e}{\partial \overline{x}} + \frac{\mu}{\rho}\frac{\partial^2 \tilde{u}}{\partial \overline{y}^2} - \frac{k_0}{\rho}\left(\tilde{u}\frac{\partial^3 \tilde{u}}{\partial \overline{x}\partial \overline{y}^2} + \tilde{v}\frac{\partial^3 \tilde{u}}{\partial \overline{y}^3} + \frac{\partial \tilde{u}}{\partial \overline{y}}\frac{\partial^2 \tilde{v}}{\partial \overline{y}^2}\right) \\ -\frac{\nu}{k}[\tilde{u} - \tilde{u}_e] - \frac{C_F}{\sqrt{k}}[\tilde{u} - \tilde{u}_e]^2 - \frac{\sigma B_0^2}{\rho}[\tilde{u} - \tilde{u}_e], \end{aligned} \tag{4}$$

$$\tilde{u}\frac{\partial T}{\partial \overline{x}} + \tilde{v}\frac{\partial T}{\partial \overline{y}} = \frac{\kappa}{\rho c_p}\frac{\partial^2 T}{\partial \overline{y}^2} - \frac{1}{\rho c_p}\frac{\partial \tilde{Q}_r}{\partial \overline{y}} + \beta K_r\left(\frac{T}{T_\infty}\right)^n e^{-\left(\frac{E_a}{KT}\right)}(C - C_\infty), \tag{5}$$

$$\tilde{u}\frac{\partial C}{\partial \overline{x}} + \tilde{v}\frac{\partial C}{\partial \overline{y}} = D_m\frac{\partial^2 C}{\partial \overline{y}^2} - K_r\left(\frac{T}{T_\infty}\right)^m e^{-\left(\frac{E_a}{KT}\right)}(C - C_\infty), \tag{6}$$

Where $\tilde{u}, \tilde{v}$ are the velocity components according to the rectangular coordinate system $\overline{x}, \overline{y}, k_0$ indicates the fluid parameter, k is the permeability of the porosity, C_F indicates the Forchheimer coefficient, σ indicates the electrical conductivity, ρ indicates the density, μ indicates the dynamics viscosity, ν indicates the kinematic viscosity, κ indicates the thermal conductivity, c_p indicates the specific heat, $\tilde{Q}_r$ indicates the radiative heat flux, $\beta(= \pm 1)$ indicates the endothermic/exothermic factor, K_r represents the chemical reaction constant, E_a the activation energy, K indicates the Boltzmann constant, m, n indicates the constant factor having the value $n \in (-1, 1)$, $K_r(T/T_\infty)^n e^{-\left(\frac{E_a}{KT}\right)}$ represents the Arrhenius expression, and D_m indicates the coefficient of mass diffusion.

The present study proposes a homogeneous-heterogeneous reactants modeling to analyze the concentrations of A and B, as depicted in the reaction pattern denoted as Eqs. (1) and (2).

$$\tilde{u}\frac{\partial a}{\partial \overline{x}} + \tilde{v}\frac{\partial a}{\partial \overline{y}} + K_c a b^2 = D_A\frac{\partial^2 a}{\partial \overline{y}^2}, \tag{7}$$

$$\tilde{u}\frac{\partial b}{\partial \overline{x}} + \tilde{v}\frac{\partial b}{\partial \overline{y}} - K_c a b^2 = D_B\frac{\partial^2 b}{\partial \overline{y}^2}. \tag{8}$$

Equations (3)–(8) are subjected to boundary conditions:

$$\begin{aligned} \tilde{u} = \tilde{u}_w(\overline{x}), \tilde{v} = \tilde{v}_w(\overline{x}), T = T_w, C = C_w, \\ D_A\frac{\partial a}{\partial \overline{y}} = K_s a, D_B\frac{\partial b}{\partial \overline{y}} = -K_s a, \text{ at } \overline{y} = 0 \\ \tilde{u} \to \tilde{u}_e(\overline{x}), \frac{\partial \tilde{u}}{\partial \overline{y}} \to 0, T \to T_\infty, C \to C_\infty, \\ a \to a_0, b \to 0 \text{ as } \overline{y} \to \infty \end{aligned} \tag{9}$$

By employing the Rosseland approximation method for thermal radiation, the heat flux attributed to radiation can be determined:

$$\tilde{Q}_r = -\frac{16\overline{\sigma}{T_\infty}^3}{3k^*}\frac{\partial T}{\partial \overline{y}}, \tag{10}$$

while k^* and $\overline{\sigma}$ represent the Rosseland mean spectral absorption coefficient and the Stefan-Boltzmann constant. We must acknowledge that we cannot ignore temperature variations within the flow. To simplify the radiative heat flux, the Taylor series expansion is applied to extend T^4 to T_∞, without considering higher-order components [42]. We get an amended version of the energy equation by plugging the model (10) into Eq. (5):

$$\tilde{u}\frac{\partial T}{\partial \bar{x}}+\tilde{v}\frac{\partial T}{\partial \bar{y}}=\frac{\kappa}{\rho c_p}\frac{\partial^2 T}{\partial \bar{y}^2}+\frac{16\bar{\sigma}{T_\infty}^3}{3k^*\rho c_p}\frac{\partial^2 T}{\partial \bar{y}^2}+\beta K_r\left[\frac{T}{T_\infty}\right]^n e^{-\left(\frac{E_a}{KT}\right)}(C-C_\infty), \tag{11}$$

It is noteworthy that the thermal radiation's nonlinear component in Eq. (5) is parameterized using the new form.

To rewrite the governing equations inside a group of nonlinear ODEs (DEs), similarity transformations are:

$$\left.\begin{aligned}\tilde{u}=c\bar{x}F'(\eta),\ \ \tilde{v}=-\sqrt{\nu c}F(\eta),\eta=\sqrt{\frac{c}{\nu}}\bar{y},G(\eta)=\frac{a}{a_0},H(\eta)=\frac{b}{a_0},\\ \theta(\eta)=\frac{T-T_\infty}{T_w-T_\infty},\phi(\eta)=\frac{C-C_\infty}{C_w-C_\infty},\end{aligned}\right\} \tag{12}$$

Additionally, the variables included in Eq. (12) satisfy Eq. (3). By inserting Eq. (12) into Eqs. (3)–(11), we get the following:

$$\begin{aligned}F'''+\Gamma_1\left[FF^{iv}+F''^2-F'F'''\right]-F'^2+FF''-F_r\left(F'^2+\lambda^2-2\lambda F'\right)\\ -\beta_D(F'-\lambda)-M(F'-\lambda)+\lambda^2=0,\end{aligned} \tag{13}$$

$$\left[1+\frac{1}{R}\right]\theta''+P_rF\theta'+P_r\beta\lambda_1\sigma_1[1+\gamma_T\theta]^n e^{-\left[\frac{E}{1+\gamma_T\theta}\right]}\phi=0, \tag{14}$$

$$\phi''+S_cF\phi'-S_c\sigma_1[1+\gamma_T\theta]^m e^{-\left[\frac{E}{1+\gamma_T\theta}\right]}\phi=0, \tag{15}$$

$$G''+Sc_A\left[FG'-K_0GH^2\right]=0, \tag{16}$$

$$\delta_1H''+Sc_B\left[FH'+K_0GH^2\right]=0. \tag{17}$$

In this investigation, we analyze the scenario involving chemical reactants that possess both homogeneous and heterogeneous characteristics, in which the diffusion coefficients of substances A and B display dissimilar diffusivities. Consequently, it is suitable to uphold the dimensionless governing Eqs. (16)–(17).

The boundary conditions reduced to:

$$F(\eta)=S,\ \ F'(\eta)\ =1,\theta(\eta)=\phi(\eta)=1,G'(\eta)=K_sG,\ \ \delta_1H'(\eta)=-K_sG,\ \ \text{at}\ \ \eta=0, \tag{18}$$

$$F'(\eta)\to\lambda,\ F''(\eta)\to 0,\theta(\eta)\to 0,\phi(\eta)\to 0,G(\eta)\to 1,\ H\to 0,\ \ \text{as}\ \ \eta\to\infty. \tag{19}$$

whereas

$$\begin{aligned}\Gamma_1=\frac{k_0c}{\rho\nu},S=-\frac{\tilde{v}}{\sqrt{c\nu}},R=\frac{3k^*\kappa}{16\bar{\sigma}{T_\infty}^3},\ \ P_r=\frac{\upsilon}{\alpha},\beta_D=\frac{\nu}{ck},F_r=\frac{C_F\tilde{u}_e}{a\sqrt{k}},M=\frac{\sigma B_0^2}{\rho c},\\ \lambda=\frac{a}{c},\sigma_1=\frac{K_r}{c},\lambda_1=\beta\left(\frac{C_w-C_\infty}{T_w-T_\infty}\right),\gamma_T=\frac{T_w-T_\infty}{T_\infty},E=\frac{E_a}{KT_\infty},S_c=\frac{\nu}{D_m},Sc_A=\frac{\nu}{D_A},\\ Sc_B=\frac{\nu}{D_B},K_0=\frac{K_c{a_0}^2}{c},K_s=\frac{K_s}{D_A\sqrt{c/\nu}},\delta_1=\frac{D_A}{D_B}.\end{aligned} \tag{20}$$

where the viscoelastic parameter is symbolized as Γ_1, S indicates the suction injection parameter, radiation parameter is given by R, P_r the Prandtl number, β_D is porosity parameter, Forchheimer number F_r demonstrates non-Darcian consequences in the porous medium, the magnetic parameter as M, λ indicates the velocity ratio parameter, σ_1, λ_1 indicates the chemical reaction rate, γ_T the temperature ration, E indicates activation energy parameter, S_c is Schmidt number, the Schmidt numbers for chemical species A and B are Sc_A, Sc_B, the strength of homogeneous and heterogeneous reactions is K_0, K_s, and the symbol δ_1 denotes the ratio of diffusion coefficient.

In the realm of engineering, there are several physical parameters that are of significant interest. Two such parameters incorporate the coefficient of shear stress, commonly referred to as the friction factor, and the local Nusselt number. The values of these parameters can be defined by utilizing the wall shear stress and heat flux, denoted as τ_w, q_w, successively. The calculations for these values can be performed using the following equations.

$$CF_{\bar{x}} = \frac{\tau_w}{\rho \tilde{u}_w^{\,2}}, Nu_{\bar{x}} = \frac{\bar{x} q_w}{\kappa(T_w - T_\infty)}, \tag{21}$$

$$\tau_w = \mu\left(\frac{\partial u}{\partial y}\right)_{y=0}, q_w = -\kappa\left(\frac{\partial T}{\partial y}\right) - \tilde{Q}_r\Big|_{y=0} \tag{22}$$

By efficiently obtaining the requisite formulae by employing the transformations mentioned in Eq. (11), we get:

$$\sqrt{\Re} CF_{\bar{x}} = F''(0), \frac{Nu_{\bar{x}}}{\sqrt{\Re}} = -\left(1 + \frac{1}{R}\right)\theta'(0) \tag{23}$$

Where $\Re(= c\bar{x}^2/\nu)$ indicates the reynolds number.

We have employed the SR method to solve the governing flow problem. Firstly, the order is reduced, so that the Gauss-Seidel relaxation approach is implemented and to decouple the contracted system. Next, the formerly estimated data is symbolized by 's' sub-components, and the newly estimated data is represented by '$s+1$', sub-components for the purpose of indexing. Then, the Chebyshev pseudo-spectral method, as described in reference [43] is applied. Numerical solutions are generated using SRM along with the Chebyshev pseudo-spectral method, spectral relaxation technique for governing flow problem. The current algorithm is formulated and implemented using the computational software MATLAB.

3. Results and discussion

Results examine the efficiency of parametric quantities for velocity $F'(\eta)$, temperature $\theta(\eta)$, and concentration profiles $\phi(\eta), G(\eta)$ and $H(\eta)$. The findings are displayed using tables and graphs. The affirmation of these outcomes is demonstrated in Table 1, which highlights the agreement of $Cf_{\bar{x}}$ values with previously published results [44–46], showing positive outcomes across different a/c values. This provides additional evidence for the numerical algorithm's accuracy. The proposed approach exhibits exceptional agreement, indicating an improved convergence. It is important to note that these findings not only showcase accuracy but also suggest that the SR methodology is an extra reliable and efficient scheme compared to other methods. Table 2 displays the numerical results of $F''(0)$ for different collocation points "N" in the SRM code. These results are obtained while keeping all other parameters constant and varying λ. Importantly, the routcomes exhibit a noteworthy stability for different collocation point quantities N. It is noted that, as λ increases, there is a significant decrease in $F''(0)$ and $-\theta'(0)$, expressing a substantial slowdown of boundary layer flow toward the stretching subsurface with a strong magnetic field employed.

Table 1. The current calculations of $F''(0)$ were compared to the previous study using the parameter a/c, while fixing $\Gamma_1 = 0, \beta_D = F_r = 0$.

a/c	Current outcomes	Mahapatra and Gupta [44]	Nazar *et al.*, [45]	Ishak *et al.*, [46]
1/10	−0.9694	−0.9694	−0.9694	−0.9694
1/5	−0.9181	−0.9181	−0.9181	−0.9181
1/2	−0.6673	−0.6673	−0.6673	−0.6673
2.0	2.0175	2.0175	2.0175	2.0175
3.0	4.7293	4.7293	4.7293	4.7293

Table 2. The SRM solution's values for $F''(0)$ for distinct λ with fixation of the other parameters.

N	λ	$F''(0)$	$-\theta'(0)$
45	0.1	−0.9672	0.7745
60	0.1	−0.9683	0.7757
70	0.1	−0.9694	0.7768
90	0.1	−0.9694	0.7768
45	0.2	−0.9160	0.7231
60	0.2	−0.9170	0.7243
70	0.2	−0.9181	0.7255
90	0.2	−0.9181	0.7255
45	0.5	−0.6651	0.4722
60	0.5	−0.6662	0.4734
70	0.5	−0.6673	0.4744
90	0.5	−0.6673	0.4744

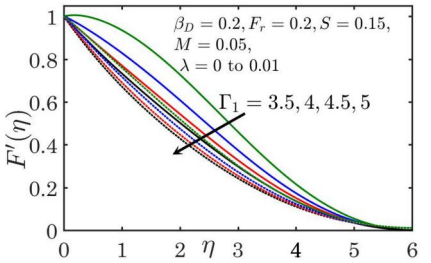


Figure 2. Fluctuation of Γ_1 and λ on $F'(\eta)$.

Figure 2 depict the influence of the viscoelastic parameter (Γ_1) and λ on the velocity profile $F'(\eta)$, for the flow. The results indicate that an increase in both (Γ_1) and λ leads to a decrease in the velocity profile. This can be explained by the heightened viscoelastic parameter, strengthening the attachment of the hydrodynamic boundary layer to the surface. The impact of the parameter (M) on the longitudinal velocity profile $F'(\eta)$ is presented in Figure 3, showing that an increase in M results in a reduction of $F'(\eta)$ due to the dominance of the Lorentz force amplifying viscous forces. Additionally, the enlargement of the parameter (S) enhances the velocity of the working fluid. Figure 4 displays the effect of β_D and F_r on velocity magnitude, indicating that as the Momentum boundary layer thickness increases, the velocity $F'(\eta)$ decreases. The permeable parameter $\beta_D = \frac{\nu}{ck}$, in eqn. (14) representing the Darcian term "$-\beta_D F'$", inversely influences the permeability of the medium and affects the velocity profile $F'(\eta)$. With an increase in β_D, there is a decrease in permeability, leading to greater resistance from solid fibers within the viscoelastic fluid. This results in a deceleration in $F'(\eta)$. An increase in Forchheimer parameter F_r leads to an escalation in $F'(\eta)$ by amplifying resistance to fluid flow across the permeable medium. This opposition encourages the fluid to navigate through narrower channels, leading to an increased fluid velocity within these pathways. As a result, the overall profile is enhanced.

The temperature function $\theta(\eta)$ is explored in Figures 5–8, illustrating the effectiveness of $R, P_r,\ \sigma_1, \beta,\ {}_1, \gamma_T,\ E$ and n. Both R and P_r exhibit a reduction in $\theta(\eta)$ as their values increase. The increase in R is associated with a slowdown in temperature in the flow range due to enhanced thermal radiation, causing a decrease in temperature distribution. Furthermore, the thickness of the thermal boundary layer decreases with an increase in P_r, reflecting the presence of P_r indicates the regulation of the comprehensive enhancement of energy and thermal boundary layers in the context of heat transfer problems. The reduction in temperature with increasing P_r is observed for both linear and nonlinear surfaces in Figure 5. P_r, being the ratio of momentum-to-thermal diffusivity, influences the heat transfer problem by controlling the thickness of energy and thermal boundary layers. In situations involving fluid metals, the thermal boundary layer is likely to be thicker than the momentum boundary layer. This is because heat diffuses more

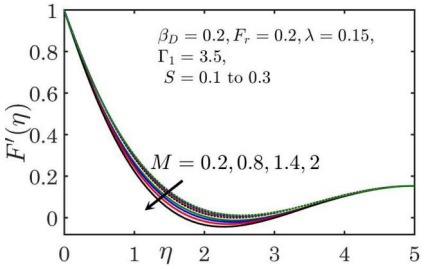


Figure 3. Fluctuation of M and S on $F^{'}$.

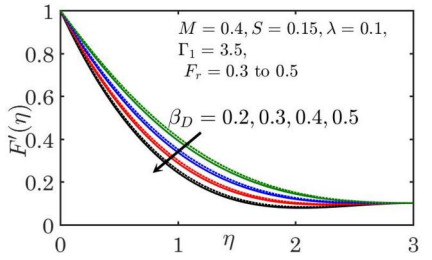


Figure 4. Fluctuation of β_D and F_r on velocity distribution.

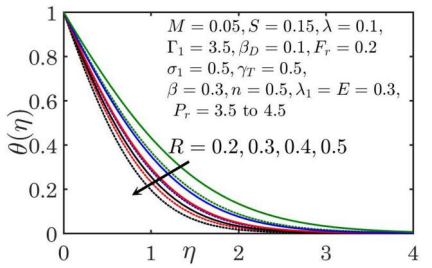


Figure 5. Fluctuation for R and P_r on temperature profiles.

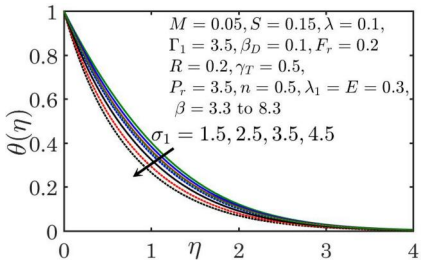


Figure 6. Alteration for σ_1 and β on temperature magnitudes.

rapidly at lower speeds in comparison to the Prandtl number. Furthermore, lower Prandtl liquids exhibit higher thermal conductivities than their greater Prandtl counterparts, facilitating faster heat diffusion through a medium. Consequently, P_r can be effectively employed to expedite the cooling process. The devaluation in temperature magnitudes is noticed as the parametric quantities $\sigma_1, \beta,\ \lambda_1,$ and γ_T escalate as depicted in Figures 6 and 7. The fluid mass moves less because of the chemical reaction. In terms of physical reality, this definition is accurate since an endothermic reaction is one that takes in energy from its surroundings, while an exothermic reaction is one that releases energy into the surrounding space. When two chemical entities interact,

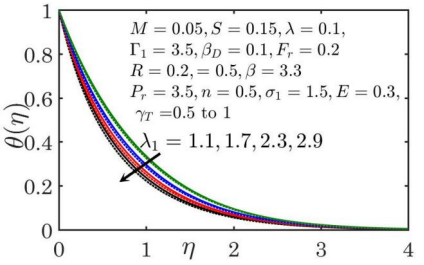


Figure 7. Impact for λ_1 and γ_T on temperature magnitudes.

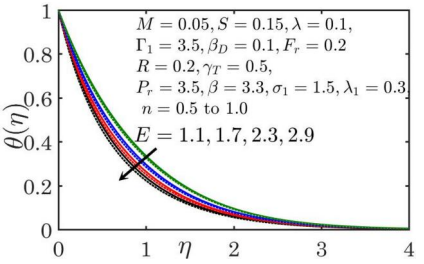


Figure 8. Impact for E and n on temperature profiles.

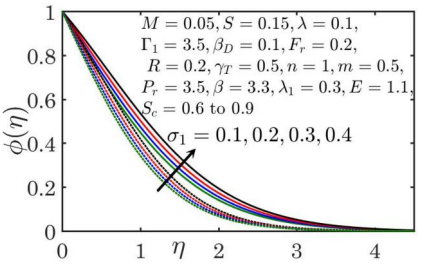


Figure 9. Impact for σ_1 and S_c on ϕ.

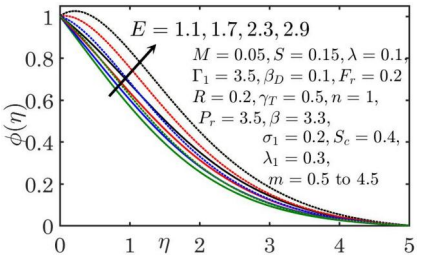


Figure 10. Impact for E and m on ϕ.

exothermic reactions result in the release of energy whereas endothermic reactions entail the absorption of energy. When this chemical process is described as isothermal, it means that the total energy is in equilibrium and the ratio of energy received to energy emitted stays constant. When the parametric values E and n increase, the temperature magnitudes decrease, as Figure 8 illustrates.

The impact of S_c, σ_1, E and m over the concentration function $\phi(\eta)$ are illustrated in Figures 9 and 10. The influence of σ_1 results in impressive escalation in $\phi(\eta)$ for larger σ_1, the reason for this phenomenon can be attributed to the direct correlation between the increment of σ_1 and

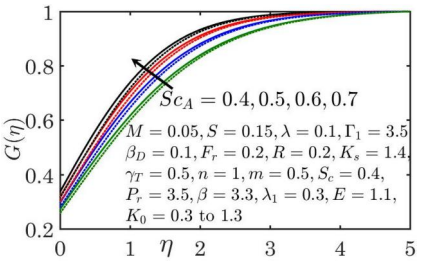


Figure 11. Influence of Sc_A and K_0 over $G(\eta)$.

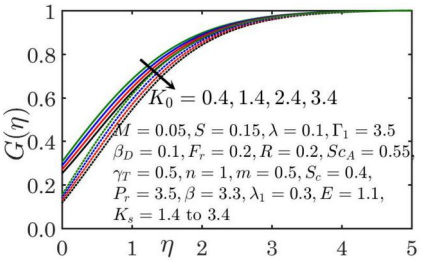


Figure 12. Alteration of K_0 and K_s on $G(\eta)$.

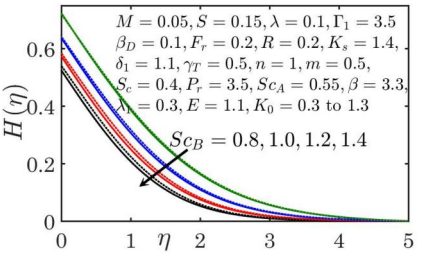


Figure 13. Alteration of Sc_B and K_0 on $H(\eta)$.

the escalation of the detrimental force exhibited by chemical reactions, while $\phi(\eta)$ decelerates across larger S_c. The observation of this phenomenon has been made due to the manifestation of increased S_c, which indicate a more pronounced manifestation of the strength of viscous diffusion rate. Furthermore, it has been observed that the rate of molecular diffusion is suppressed. Figure 10 illustrates the enhancement of the $\phi(\eta)$ as the activation energy parameter E increases, and $\phi(\eta)$ also escalates as m increases.

Figures 11 depicts the concentration of species A, concerning the ratio of momentum diffusivity to mass diffusivity $Sc_B = 0.55$, and the magnitudes of homogeneous-heterogeneous reactions "$K_s = 1.4$". The data indicates that $G(\eta)$ increases with an increase in Sc_A, while it is deduced that an elevation in the numerical value of K_0 leads to a substantial reduction in $G(\eta)$. The figure depicted in Figure 12 illustrates the behavior of $G(\eta)$, as K_0 and K_s heighten. The concentration $G(\eta)$ demonstrates slight decrement for K_0, which is only apparent adjacent the walls. Conversely, near the wall, $G(\eta)$ experiences an obvious decrement across K_s. The species B to $Sc_A = 0.55$, $H(\eta)$ decreases for the escalated numeric in Sc_B, and has an obvious escalation across K_0 on $H(\eta)$ as depicted in Figure 13. The impact of Sc_B, and δ_1 over $H(\eta)$ as depicted in Figure 14 demonstrates a significant deceleration for both, respectively. This significant reduction can be attributed to the value assigned to the parameter δ_1. The notable reduction in impact is attributable to the quantification attributed to parameter δ_1. This explains why δ_1 does not exert

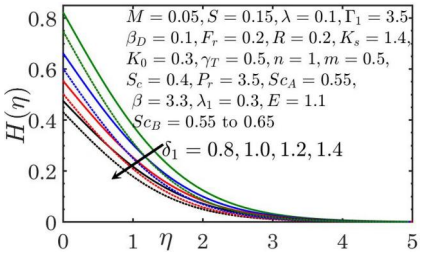


Figure 14. Influence of δ_1 and Sc_B over $H.\ (\eta)$

a significant influence on the concentration of chemical species $H(\eta)$ due to the fixed magnitudes of K_0 and K_s.

4. Concluding remarks

The goal of this study was to show how a magnetic field and nonlinear thermal radiation can change the flow properties of a viscous, incompressible fluid near a stopping point in a non-Darcian permeable medium by using computer simulations. To get numerical solutions, the system of coupled nonlinear differential equations is solved using the Spectral Relaxation Method (SRM) technique. The governing equations of fluid flow and the related boundary conditions are successfully addressed by the current method. Visual representations of the obtained results are shown, and a comparison is made between these results and the outcomes of an earlier investigation. Many important findings have been drawn from the present inquiry, some of which are summarized below:

i. The existence of parameter M causes to a reduction in the magnitude of velocity field.
ii. An upsurge in the parameters Γ_1, λ results in lowering the velocity profile.
iii. Increasing the parameter S accelerates the flow in in $F'(\eta)$.
iv. The velocity $F'(\eta)$ experiences both a decrease and increase with variations in the parametric quantities of β_D and F_r, subsequently.
v. The temperature function $\theta(\eta)$ undergoes a reduction with raising in the magnitude of both R and P_r.
vi. A decrement in temperature is observed as the parameters he reduction in temperature is observed as the $\sigma_1, \beta,\ \lambda_1, \gamma_T,\ E$ and n escalate.
vii. An impressive escalation in $\phi(\eta)$ for larger σ_1, while $\phi(\eta)$ decelerates across larger S_c.
viii. The $\phi(\eta)$ enhances across the enlarging numeric of both E and m.
ix. $G(\eta)$ increases for larger Sc_A, and decreases across enlarging numeric of K_s and K_0.
x. The concentration $H(\eta)$ exhibits decrement with enlarger numeric in Sc_B. A higher numerical value of K_0 leads to an increase in $H(\eta)$.
xi. Elevated values of the strength in δ_1 result in a respective deceleration in $H(\eta)$.
xii. The SRM approach shows exceptional accuracy and numerical resilience in addressing nonlinear boundary value problems in the domain of multi-physical reactive magnetic rheological nanofluid-coated materials processing over complicated surfaces.

Disclosure statement

No potential conflict of interest was reported by the authors.

ORCID

Anwar Shahid http://orcid.org/0000-0003-2702-6457
M. M. Bhatti http://orcid.org/0000-0002-3219-7579

Data availability statement

The information about data availability is not applicable to this article since no datasets were generated or analyzed during the current study.

References

[1] R. C. Bataller, "Viscoelastic fluid flow and heat transfer over a stretching sheet under the effects of a non-uniform heat source, viscous dissipation and thermal radiation," *Int. J. Heat Mass Transf*, vol. 50, no. 15-16, pp. 3152–3162, 2007. DOI: 10.1016/j.ijheatmasstransfer.2007.01.003.

[2] V. Singh and S. Agarwal, "Heat transfer for two types of viscoelastic fluid over an exponentially stretching sheet with variable thermal conductivity and radiation in porous medium," *Therm Sci*, vol. 18, no. 4, pp. 1079–1093, 2014. DOI: 10.2298/TSCI111102144S.

[3] M. H. Abolbashari, N. Freidoonimehr, F. Nazari and M. M. Rashidi, "Analytical modeling of entropy generation for Casson nano-fluid flow induced by a stretching surface," *Adv. Powder Technol*, vol. 26, no. 2, pp. 542–552, 2015. DOI: 10.1016/j.apt.2015.01.003.

[4] S. K. Adegbie, O. K. Koṛikọ and I. L. Animasaun, "Melting heat transfer effects on stagnation point flow of micropolar fluid with variable dynamic viscosity and thermal conductivity at constant vortex viscosity," *J. Nigerian Math. Soc*, vol. 35, no. 1, pp. 34–47, 2016. DOI: 10.1016/j.jnnms.2015.06.004.

[5] N. Sandeep, C. Sulochana and I. L. Animasaun, "Stagnation-point flow of a Jeffrey nanofluid over a stretching surface with induced magnetic field and chemical reaction," *JERA*, vol. 20, pp. 93–111, 2015. DOI: 10.4028/www.scientific.net/jera.20.93.

[6] H. Emad and I. Aly, "MHD flow and heat transfer near stagnation point over a stretching/shrinking surface with partial slip and viscous dissipation: hybrid nanofluid versus nanofluid," *Powder Technol.*, vol. 367, pp. 192–205, 2020. DOI: 10.1016/j.powtec.2020.03.030.

[7] W. Ibrahim and A. Tulu, "Magnetohydrodynamic (MHD) boundary layer flow past a wedge with heat transfer and viscous effects of nanofluid embedded in porous media," *Math. Probl. Eng*, vol. 2019, pp. 1–12, 2019. DOI: 10.1155/2019/4507852.

[8] K. Ramesh, S. U. Khan, M. Jameel, M. I. Khan, Y.-M. Chu and S. Kadry, "Bioconvection assessment in Maxwell nanofluid configured by a Riga surface with nonlinear thermal radiation and activation energy," *Surf. Interfaces*, vol. 21, no. 100749, pp. 100749, 2020. DOI: 10.1016/j.surfin.2020.100749.

[9] M. Ramana, R. Venkateswara Raju and K. G. Kumar, "Multiple slips and heat source effects on MHD stagnation point flow of Casson fluid over a stretching sheet in the presence of chemical reaction," *Materials: Today: Proc.*, vol. 49, no. 5, pp. 2306–2315, 2022. DOI: 10.1016/j.matpr.2021.09.348.

[10] M. M. Khader and M. M. Babatin, "Numerical study for improvement the cooling process through a model of Powell-Eyring fluid flow over a stratified stretching sheet with magnetic field," *Case Stud. Therm. Eng.*, vol. 31, no. 101786, pp. 101786, 2022. DOI: 10.1016/j.csite.2022.101786.

[11] I. Ahmed, M. Alghamdi, M. Amjad, F. Aziz, T. Akbar and T. Muhammad, "Numerical investigation of MHD flow of hyperbolic tangent nanofluid over a non-linear stretching sheet," *Heliyon*, vol. 9, no. 7, pp. e17658, 2023. DOI: 10.1016/j.heliyon.2023.e17658.

[12] O. D. Makinde, P. O. Olanrewaju and W. M. Charles, "Unsteady convection with chemical reaction and radiative heat transfer past a flat porous plate moving through a binary mixture," *Afr. Mat*, vol. 22, no. 1, pp. 65–78, 2011. DOI: 10.1007/s13370-011-0008-z.

[13] Aamir, Hamid, Masood, Khan, Hashim, "Impacts of binary chemical reaction with activation energy on unsteady flow of magneto-Williamson nanofluid," *J. Mol. Liq.*, vol. 262, pp. 435–442, 2018, DOI: 10.1016/j.molliq.2018.04.095.

[14] M. Irfan, W. A. Khan, M. Khan and M. M. Gulzar, "Influence of Arrhenius activation energy in chemically reactive radiative flow of 3D Carreau nanofluid with nonlinear mixed convection," *J. Phys. Chem. Solids*, vol. 125, pp. 141–152, 2019. DOI: 10.1016/j.jpcs.2018.10.016.

[15] A. Abbasi, *et al.*, "Thermal decomposition of hybrid nanofluid confined by radiated curved stagnated surface capturing partial slip effects," *Results Eng*, vol. 19, no. 101393, pp. 101393, 2023. DOI: 10.1016/j.rineng.2023.101393.

[16] M. M. Bhatti and E. E. Michaelides, "Study of Arrhenius activation energy on the thermo-bioconvection nanofluid flow over a Riga plate," *J Therm Anal Calorim*, vol. 143, no. 3, pp. 2029–2038, 2021. DOI: 10.1007/s10973-020-09492-3.

[17] M. M. Bhatti, O. A. Bég and S. Kuharat, "Electromagnetohydrodynamic (EMHD) convective transport of a reactive dissipative Carreau fluid with thermal ignition in a non-Darcian vertical duct," *Numer. Heat Transf. A*, pp. 1–31, 2023. DOI: 10.1080/10407782.2023.2284333.

[18] N. Sandeep, C. Sulochana and B. R. Kumar, "MHD boundary layer flow and heat transfer past a stretching/shrinking sheet in a nanofluid," *J Nanofluids*, vol. 4, no. 4, pp. 512–517, 2015. DOI: 10.1166/jon.2015.1181.

[19] N. Sandeep, C. S. K. Raju, C. Sulochana and V. Sugunamma, "Effects of aligned magnetic field and radiation on the flow of ferrofluids over a flat plate with non-uniform heat source/sink," *Int. J. Sci. Eng*, vol. 8, no. 2, pp. 151–158, 2015. DOI: 10.12777/ijse.8.2.151-158.

[20] I. L. Animasaun, "Dynamics of unsteady MHD convective flow with thermophoresis of particles and variable Thermo-physical properties past a vertical surface moving through binary mixture," *OJFD*, vol. 05, no. 02, pp. 106–120, 2015. DOI: 10.4236/ojfd.2015.52013.

[21] A. Wakif, Z. Boulahia, F. Ali, M. R. Eid and R. Sehaqui, "Numerical analysis of the unsteady natural convection MHD couette nanofluid flow in the presence of thermal radiation using single and two-phase nanofluid models for cu–water nanofluids," *Int. J. Appl. Comput. Math*, vol. 4, no. 3, pp. 81, 2018. DOI: 10.1007/s40819-018-0513-y.

[22] M. S. Kausar, M. Waqas, S. A. Shehzad, K. Hosseinzadeh, H. A. Hejazi and W. Mtaouaa, "Numerical computations for Darcy–Forchheimer-based dual convection reactive flow considering Casson nanomaterial by convected permeable surface," *Int. J. Mod. Phys. B*, 2024. DOI: 10.1142/S0217979224504265.

[23] M. Waqas, *et al.*, "Numerical study of dissipative SW/MWCNT-nanofluid coating flow from a stretching wall to a porous medium with shape factor effects," *Int. J. Hydrogen Energy*, vol. 48, no. 88, pp. 34536–34550, 2023. DOI: 10.1016/j.ijhydene.2023.05.036.

[24] A. S. Oke, "Coriolis effects on MHD flow of MEP fluid over a non-uniform surface in the presence of thermal radiation," *Int. Commun. Heat Mass Transf*, vol. 129, no. 105695, pp. 105695, 2021. DOI: 10.1016/j.icheatmasstransfer.2021.105695.

[25] S. Mishra, B. Mahanthesh, J. Mackolil and P. K. Pattnaik, "Nonlinear radiation and cross-diffusion effects on the micropolar nanoliquid flow past a stretching sheet with an exponential heat source," *Heat Trans*, vol. 50, no. 4, pp. 3530–3546, 2020. no. htj.22039, DOI: 10.1002/htj.22039.

[26] M. Izadi, M. A. Sheremet and S. A. M. Mehryan, "Natural convection of a hybrid nanofluid affected by an inclined periodic magnetic field within a porous medium," *Chin. J. Phys*, vol. 65, pp. 447–458, 2020. DOI: 10.1016/j.cjph.2020.03.006.

[27] M. R. Eid and M. A. Nafe, "Thermal conductivity variation and heat generation effects on magneto-hybrid nanofluid flow in a porous medium with slip condition," *Waves Random Complex Media*, vol. 32, no. 3, pp. 1103–1127, 2022. DOI: 10.1080/17455030.2020.1810365.

[28] Z. Ying, B. He, L. Su and Y. Kuang, "Thermo-hydraulic analyses of the absorber tube with molten salt-based nanofluid and porous medium inserts," *Sol. Energy*, vol. 226, pp. 20–30, 2021. DOI: 10.1016/j.solener.2021.08.021.

[29] K. Loganathan, N. Alessa, K. Tamilvanan and F. S. Alshammari, "Significances of Darcy-Forchheimer porous medium in third-grade nanofluid flow with entropy features," *Eur. Phys. J. Spec. Top*, vol. 230, no. 5, pp. 1293–1305, 2021. DOI: 10.1140/epjs/s11734-021-00056-6.

[30] B. Mohanty, S. Mohanty, S. R. Mishra and P. K. Pattnaik, "Analysis of entropy on the peristaltic transport of micropolar nanofluid: a simulation obtained using approximate analytical technique," *Eur. Phys. J. Plus*, vol. 136, no. 11, pp. 1139, 2021. DOI: 10.1140/epjp/s13360-021-02150-z.

[31] P. C. Pattanaik, S. R. Mishra, S. Jena and P. K. Pattnaik, "Impact of radiative and dissipative heat on the Williamson nanofluid flow within a parallel channel due to thermal buoyancy," *Proc. Inst. Mech. Eng. N J. Nanomater. Nanoeng. Nanosyst*, vol. 236, no. 1-2, pp. 3–18, 2022. DOI: 10.1177/23977914221080046.

[32] M. R. Eid, "Thermal characteristics of 3D nanofluid flow over a convectively heated Riga surface in a Darcy-Forchheimer porous material with linear thermal radiation: an optimal analysis," *Arab J Sci Eng*, vol. 45, no. 11, pp. 9803–9814, 2020. DOI: 10.1007/s13369-020-04943-3.

[33] M. M. Bhatti, I. Sarris, E. E. Michaelides and R. Ellahi, "Sisko fluid flow through a non-Darcian microchannel: an analysis of quadratic convection and electro-magneto-hydrodynamics," *Therm. Sci. Eng. Prog*, vol. 50, no. 102531, pp. 102531, 2024. DOI: 10.1016/j.tsep.2024.102531.

[34] M. El Maghraoui, R. Mohebbi, M. Sheremet and M. Hazami, "Simulation of conductive fins effect on mixed convection heat transfer in a two-dimensional inclined channel using the lattice Boltzmann method," *Numer. Heat Transf. A*, vol. 85, no. 7, pp. 1130–1156, 2024. DOI: 10.1080/10407782.2023.2197266.

[35] J. H. Merkin, "A model for isothermal homogeneous-heterogeneous reactions in boundary-layer flow," *Math. Comput. Model*, vol. 24, no. 8, pp. 125–136, 1996. DOI: 10.1016/0895-7177(96)00145-8.

[36] F. Mabood, W. A. Khan and A. I. M. Ismail, "MHD stagnation point flow and heat transfer impinging on stretching sheet with chemical reaction and transpiration," *Chem. Eng. J*, vol. 273, pp. 430–437, 2015. DOI: 10.1016/j.cej.2015.03.037.

[37] I. L. Animasaun, "Effects of thermophoresis, variable viscosity and thermal conductivity on free convective heat and mass transfer of non-Darcian MHD dissipative Casson fluid flow with suction and nth order of chemical reaction," *J. Nigerian Math. Soc*, vol. 34, no. 1, pp. 11–31, 2015. DOI: 10.1016/j.jnnms.2014.10.008.

[38] W. A. Khan and I. M. Pop, "Effects of homogeneous–heterogeneous reactions on the viscoelastic fluid toward a stretching sheet," *J. Heat Transfer*, vol. 134, no. 6, pp. 064506, 2012. DOI: 10.1115/1.4006016.

[39] M. R. Eid, K. L. Mahny and A. F. Al-Hossainy, "Homogeneous-heterogeneous catalysis on electromagnetic radiative Prandtl fluid flow: Darcy-Forchheimer substance scheme," *Surf. Interfaces*, vol. 24, no. 101119, pp. 101119, 2021. DOI: 10.1016/j.surfin.2021.101119.

[40] Hina, Zahir, Javaria, Akram, Mehnaz, Reem K., Alhefthi, Rabbia, Fatima, Mustafa Inc, "Effect of nonlinear thermal radiation and homogeneous-heterogeneous reactions on peristaltic propulsion of Johnson-Segalman fluid," *Ain Shams Eng. J.*, vol. 15, no. 2, p. 102383, 2024, DOI: 10.1016/j.asej.2023.102383.

[41] I. L. Animasaun, C. S. K. Raju and N. Sandeep, "Unequal diffusivities case of homogeneous–heterogeneous reactions within viscoelastic fluid flow in the presence of induced magnetic-field and nonlinear thermal radiation," *Alex. Eng. J*, vol. 55, no. 2, pp. 1595–1606, 2016. DOI: 10.1016/j.aej.2016.01.018.

[42] L. Zhang, N. Tariq and M. M. Bhatti, "Study of nonlinear quadratic convection on magnetized viscous fluid flow over a non-Darcian circular elastic surface via spectral approach," *J. Taibah Univ. Sci.*, vol. 17, no. 1, 2183702, 2023. DOI: 10.1080/16583655.2023.2183702.

[43] L. N. Trefethen, *Spectral Methods in MATLAB, Volume 10 of Software, Environments, and Tools*. Philadelphia, PA: Society for Industrial and Applied Mathematics (SIAM), 2000, pp. 24.

[44] T. R. Mahapatra and A. S. Gupta, "Stagnation-point flow of a viscoelastic fluid towards a stretching surface," *Int. J. Non Linear Mech.*, vol. 39, no. 5, pp. 811–820, 2004. DOI: 10.1016/s0020-7462(03)00044-1.

[45] R. Nazar, N. Amin, D. Filip and I. Pop, "Unsteady boundary layer flow in the region of the stagnation point on a stretching sheet," *Int. J. Eng. Sci.*, vol. 42, no. 11-12, pp. 1241–1253, 2004. DOI: 10.1016/j.ijengsci.2003.12.002.

[46] A. Ishak, R. Nazar and I. Pop, "Mixed convection boundary layers in the stagnation-point flow toward a stretching vertical sheet," *Meccanica*, vol. 41, no. 5, pp. 509–518, 2006. DOI: 10.1007/s11012-006-0009-4.